1   *Saccharomyces cerevisiae* histone Chaperones FACT and Spt6 modulate Pol II and histone

2   occupancy genome-wide

3

4   **Rakesh Pathak[1], Priyanka Singh[1], Sudha Ananthakrishnan[1], Sarah Adamczyk[1], Olivia**

5   **Schimmel[1] and Chhabi K. Govind[1, #]**

6

7   [1] Department of Biological Sciences

8   Oakland University

9   Rochester

10   Michigan, USA.

11

14

15

16

17

18

19

20

21

22

23

24

Running title: FACT and Spt6 regulate transcription and chromatin

26

Key words: Spt6, Spt16, FACT, transcription elongation, histone chaperones, Gcn4,

Saccharomyces cerevisiae, Gcn5, Esa1, histone acetyltransferases, genome-wide, ChIP-chip.

29

Corresponding author: Chhabi K. Govind

Department of Biological Sciences

Mathematics and Science Center (MSC)

Room number 333, Oakland University, Rochester, MI-48085, USA

Tel: 248-270-2027

e-mail: govind@oakland.edu

36

37

38

39

40

41

42

43

44

45

46

ABSTRACT

Histone chaperones, chromatin remodelers, and histone modifying complexes play a critical role in alleviating the nucleosomal barrier. Here, we have examined the role of two highly conserved yeast (*Saccharomyces cerevisiae*) histone chaperones, FACT and Spt6, in regulating transcription and histone occupancy. We show that the H3 tail contributes to the recruitment of FACT to coding sequences in a manner dependent on acetylation. We found that deleting a H3 HAT Gcn5 or mutating lysines on the H3 tail impairs FACT recruitment at *ADH1* and *ARG1* genes. However, deleting the H4 tail or mutating the H4 lysines failed to dampen FACT occupancy in coding regions. Additionally, we show that FACT-depletion greatly reduces Pol II occupancy in the 5' ends genome-wide. By contrast, Spt6-depletion led to reduction in Pol II occupancy towards the 3' end, in a manner dependent on the gene-length. Severe transcription and histone eviction defects were also observed in a strain that was impaired for Spt6 recruitment (*spt6Δ202*) and depleted of FACT. Importantly, the severity of the defect strongly correlated with WT Pol II occupancies at these genes, indicating critical roles of Spt6 and Spt16 in promoting high-level transcription. Collectively, our study shows cooperation, as well as redundancy between chaperones, FACT and Spt6, in regulating transcription and chromatin in coding regions of transcribed genes.

64

65

66

67

68   **INTRODUCTION**

69   The nucleosome is the fundamental unit of chromatin and is composed of ~ 147 bp of

70   DNA wrapped around a histone octamer consisting of two copies of histones H2A, H2B, H3 and

71   H4. Nucleosomes pose a significant impediment to all steps of transcription, including the steps

72   of initiation and elongation of RNA polymerase II (Pol II) through the coding sequences (CDS)

73   (LI *et al.* 2007). There are two principle mechanisms suggested to alleviate nucleosomal barrier:

74   I) removal of the H2A-H2B dimer to generate hexamers that can be readily overcome by

75   elongating polymerases (KIREEVA *et al.* 2002), and II) complete removal of histone octamers

76   leading to reduced nucleosomal density across the transcribing genes (LEE *et al.* 2004; DION *et*

77   *al.* 2007).

78   Various factors and enzyme complexes have been implicated in removing the nucleosomal

79   barriers *in vivo* (LI *et al.* 2007). For example, acetylation of histone tails facilitates histone

80   eviction by weakening histone-DNA interactions (GOVIND *et al.* 2007; GOVIND *et al.* 2010) and

81   by promoting recruitment of ATP-dependent remodelers, such as RSC and SWI/SNF (HASSAN *et*

82   *al.* 2001; DECHASSA *et al.* 2010; SPAIN *et al.* 2014). While nucleosome disassembly is important

83   for transcription, it is also important to restore the chromatin structure in the wake of

84   transcription. Histone chaperones, many of which are cotranscriptionally recruited to actively

85   transcribing genes, are implicated in performing this function (GURARD-LEVIN *et al.* 2014).

86   Two such chaperones, the FACT complex (Spt16/SSRP1 in humans and Spt16/Pob3 in

87   yeast) and Spt6, are enriched in transcribed coding regions (ANDRULIS *et al.* 2000; KAPLAN *et al.*

88   2000; KROGAN *et al.* 2002; MASON AND STRUHL 2003; MAYER *et al.* 2010; FORMOSA 2012;

89   BURUGULA *et al.* 2014), suggesting a role for these factors in regulating transcription and in

90   maintaining chromatin integrity. Human FACT recognizes and displaces one of the H2A/H2B

91   dimers from the nucleosome, and promotes transcription on a chromatin template, *in vitro*. In

92   addition, it can assemble all four histones on the DNA (BELOTSERKOVSKAYA *et al.* 2003). Yeast

93   (*S. cerevisiae*) FACT also interacts with all four histones and displays a strong affinity toward

94   intact nucleosomes (FORMOSA *et al.* 2001; VANDEMARK *et al.* 2008). Multiple domains within

95   the FACT subunits Spt16 and Pob3 are implicated in binding and chaperoning histones

96   (HONDELE AND LADURNER 2011; FORMOSA 2012). The N-terminal domain (peptidase-like) of *S.*

97   *pombe* Spt16, for example, binds to both core histones as well as histone N-terminal tails

98   (STUWE *et al.* 2008), and the M-domain of *Chaetomium thermophilum* Spt16 recognized

99   H2A/H2B with affinity similar to that observed with full-length Spt16 (HONDELE *et al.* 2013).

100   However, in *S. cerevisiae*, the C-terminal regions of both Spt16 and Pob3 were defined as

101   H2A/H2B binding domains (VANDEMARK *et al.* 2008; KEMBLE *et al.* 2015). Whether these

102   different domains are required for interacting with nucleosomes in a context-dependent manner

103   remains to be seen.

104   FACT is shown to promote reassembly of the displaced H3/H4 in the *ADH1*, *ADH2* and

105   *STE3* coding regions (JAMAI *et al.* 2009) implicating FACT in restoring chromatin behind

106   elongating Pol II. The role of FACT (and Spt6) in regulating histone occupancy has been

107   examined at a genome-wide scale (VAN BAKEL *et al.* 2013; JERONIMO *et al.* 2015). Impairing

108   FACT function leads to reduced histone occupancy and also results in aberrant incorporation of a

109   histone variant H2AZ (JERONIMO *et al.* 2015). Additionally, recruitment of FACT to the *HO*

110   promoter is shown to promote histone eviction (TAKAHATA *et al.* 2009). Likewise, FACT helps

111   in evicting H2A/H2B from the promoter of the PHO5 gene, upon induction (RANSOM *et al.*

112   2009).

113   Gene-specific studies have shown a role for FACT in regulating transcription. For

114   example, FACT mutants impaired Pol II and TBP recruitment at the *GAL1* promoter, implicating

115   a role for FACT in regulating transcription at the initiation step (BISWAS *et al.* 2006; FLEMING *et*

116   *al.* 2008). However, moderate reductions in Pol II occupancy were observed in the 3' ORFs of

117   *GAL1* and *PHO5* but not in *LacZ* or *YAT1* genes expressed on plasmids under the control of

118   *GAL1* promoter (JIMENO-GONZALEZ *et al.* 2006). Likewise, transcription defects were observed

119   only at *ADH1* and not at *ADH2* or *STE3*, despite all three genes showing a histone reassembly

120   defect (JAMAI *et al.* 2009), making it unclear if FACT is generally required for transcription. In

121   addition to transcription initiation, FACT is shown to participate in promoting Pol II processivity

122   and elongation rate at *GAL1* gene, in conjunction with the H2B ubiquitination (FLEMING *et al.*

123   2008).

124   FACT shares many functional similarities with another histone chaperone, known as

125   Spt6, which interacts with H3/H4 (KAPLAN *et al.* 2003; MAYER *et al.* 2010), and also with

126   H2A/H2B (MCCULLOUGH *et al.* 2015). Loss of Spt6 function leads to reduced histone occupancy

127   over transcribed regions, suggesting a role for Spt6 in cotranscriptional histone reassembly

128   (IVANOVSKA *et al.* 2011; PERALES *et al.* 2013; VAN BAKEL *et al.* 2013; JERONIMO *et al.* 2015).

129   Spt6, along with the FACT complex, is also implicated in preventing spurious incorporation of

130   H2AZ in coding regions (JERONIMO *et al.* 2015) and thereby helps in restricting H2AZ to

131   promoter nucleosomes (BILLON AND COTE 2013). Therefore, Spt6 and FACT play important

132   roles in maintaining chromatin integrity. Consistent with this, widespread aberrant transcription

133   was observed in the cells deficient of Spt6 or FACT (CHEUNG *et al.* 2008; VAN BAKEL *et al.*

134   2013).

135   Spt6 mutants have also been shown to alter histone modifications and reduce

136   transcription genome-wide (DEGENNARO *et al.* 2013; KATO *et al.* 2013; PERALES *et al.* 2013).

137   Spt6 possesses a tandem SH2 (tSH2) domain at its C-terminus that interacts with phosphorylated

138   Pol II CTD, *in vitro* (DENGL *et al.* 2009; CLOSE *et al.* 2011; LIU *et al.* 2011) and this domain is

139   implicated in promoting Spt6 recruitment to transcribed genes, *in vivo* (MAYER *et al.* 2010;

140   MAYER *et al.* 2012; BURUGULA *et al.* 2014).

141   In this study, we show that the acetylated histone H3 tail contributes to efficient

142   recruitment of FACT to transcribed coding sequences in *S. cerevisiae*. Depleting Spt16 subunit

143   of FACT elicits a greater reduction in Pol II occupancies in the 5'ends of the genes, suggesting a

144   potential role for FACT in the early elongation steps of transcription. In contrast, Pol II

145   occupancies were reduced more towards the 3' end in Spt6-depleted cells, suggestive of

146   processivity defects. Together, our results suggest a spatial regulation of transcription by these

147   two highly conserved histone chaperones. Importantly, depleting Spt16 in a strain compromised

148   for Spt6 recruitment evoked severe defects in transcription and histone eviction, suggesting that

149   these chaperones may cooperate to promote a high-level transcription by modulating histone

150   occupancies across transcribed genes.

151

152   **MATERIALS AND METHODS**

153   *Yeast strains and growth conditions*

154   The yeast strains used in this study are listed in Table S1. The cells were grown to absorbance

155   A_{600} of 0.5-0.6 in synthetic complete (SC) media lacking isoleucine/valine, and treated with

156   sulfometuron methyl (SM; 0.6 μg/ml) for 30 minutes to induce Gcn4 targets. Esa1 in the

157   *gcn5Δ/esa1ts* strain was inactivated by shifting the cultures grown at 25°C to 37°C for ~1.5

158   hours prior to induction by SM. Spt16 and Spt6 were depleted in *SPT16-TET* and *SPT6-TET*

159   (HUGHES *et al.* 2000; MNAIMNEH *et al.* 2004) cells by growing these strains in the presence of 10

160   μg/ml doxycycline overnight, and sub-culturing the overnight cultures in 100 ml of synthetic

161   complete (SC) media with 10 μg/ml doxycycline to an OD_{600} of 0.6.

162

163   *Coimmunoprecipitation Assay*

164   The coimmunoprecipitation experiments were performed as described previously (GOVIND *et al.*

165   2010). The HA-tagged H2B or Spt16-Myc tagged WT and *H3Δ1-28* strains were resuspended in

166   500 μl of lysis buffer (50 mM Tris-HCl [pH-7.5], 50 mM HEPES-KOH [pH 7.9], 10 mM

167    $MgSO_4$, 100 mM $(NH_4)_2SO_4$, 12.5 mM KOAc, 0.01% NP-40, 20% Glycerol, 1ug/ml Pepstatin

168   A, 100 mM PMSF, 1ug/ml Leupeptin;) and 500 μl of glass beads, and disrupted by vortexing (18

169   seconds x 8 times, and 150 seconds on ice between each agitation cycle). Whole cell extracts

170   were incubated overnight with magnetic beads that were pre-conjugated to anti-Myc or anti-HA

171   antibodies in 100 μl 4X MTB buffer (200 mM HEPES-KOH [pH 7.9], 800 mM KOAc, 54 mM

172   MgOAc2, 40% Glycerol, 0.04% NP-40, 400 mM PMSF, 4 ug/ml Pepstatin, 4ug/ml Leupeptin),

173   and washed 5 times with the wash buffer (50 mM Tris-HCl (pH-8.0), 0.3% NP-40, 500 mM

174   NaCl, 10% Glycerol, 1mM PMSF, 1ug/ml Leupeptin, and 1ug/ml Pepstatin).

175   Immunoprecipitates were analyzed by western blot using the following antibodies: anti-Myc

176   (Roche), anti-HA (Roche), anti-Spt16 and anti-Spt6 antibodies (kindly provided by Tim

177   Formosa). The signal intensities were quantified using Image Studio lite version 5.2 (LI-COR

178   Biosciences).

179

180   *ChIP and ChIP-chip*

181   The cultures were crosslinked with formaldehyde and processed for chromatin

182   immunoprecipitation as described previously (GOVIND et al. 2012). ChIPs were performed using

183   antibodies, anti-Myc (Roche), anti-Rpb3 (Neoclone), and anti-H3 (Abcam). ChIP DNA and the

184   related input DNA was amplified using the primers against specific regions. 5μl of ChIP dye

185   (15% Ficol, 0.25% bromophenol blue in 1X TBE) and SYBR green dye were added in the PCR

186   products, resolved on 8% TBE gels and visualized on a phosphorimager and quantified using

187   ImageQuant 5.1 software. The fold enrichments were determined by taking the ratios of the ChIP

188   signal for gene of interest, and the signal obtained for the *POL1* used as an internal control and

189   dividing by the ratios obtained for the related input samples (ChIP/Input fold enrichment: ChIP

190   intensities [*ARG1/POL1*]) / input intensities [*ARG1/POL1*]). The ChIP experiments were

191   performed using at least three independent cultures, and PCR reactions were conducted at least

192   in duplicates. The error bars represent standard error of mean (SEM).

193   For ChIP-chip experiments, ChIP and related input DNA samples were amplified, from at least

194   two biological replicates, using the GenomePlex complete whole genome amplification (WGA)

195   kit (Sigma, cat # WGA2), according to the manufacturer's instructions. The amplified ChIP

196   DNA and input DNA were purified by using PCR cleanup kit (Qiagen Cat # 28104) and the

197   DNA was quantified by NanoDrop. The samples were hybridized on Agilent 4x44 arrays

198   (G4493A) after labeling the ChIP and input DNA with Alexa555 and Alexa647 fluorescent dyes,

199   respectively, as per the manufacturer's instructions at genomic core facility at Michigan State

200   University. The arrays were scanned using Agilent scanner, and data was extracted with the

201   Feature Extraction software (Agilent) as described previously (SPAIN et al. 2014).

202

203   *Bioinformatics Analysis*

204   The data extracted with the Feature Extraction software (Agilent) was normalized using Limma

205   package from Bioconductor, as described previously (VENKATESH *et al.* 2012). The genes were

206   divided into 10 equal sized bins, with the two bins assigned to the region 500 bp upstream of the

207   transcription start site (TSS) and two bins to the 500 bp to the region downstream of the

208   transcription end site (TES). The average probe enrichment values were assigned to the closest

209   bin according to the probe location, and a 10 bin matrix was generated using a PERL script.

210   Genes corresponding to the majority of dubious ORFs, tRNA genes, small nuclear RNA genes as

211   well as autonomously replicating sequences (ARS) were removed from the dataset. The

212   enrichments in the 6 bins between TSS and TES were averaged to obtain an average ORF

213   occupancy. The genes for analysis were selected on the basis of ORF enrichment. The genes

214   <500 bp in length were removed from the analyses. The versatile aggregate profiler (BRUNELLE

215   *et al.* 2015) was used to generate gene-average profile. The genes were split in the middle, and

216   the probe intensities were aligned to the TSS for the first half and to the TES for the second half

217   of the genes.

218

219   *Box-plots*

220   Center lines show the median and box limits indicate the 25th and 75th percentiles as determined

221   by R software. Whiskers extend 1.5 times the interquartile range from the 25th and 75th

222   percentiles and outliers are represented by dots.

223

224   *Data Availability*

10

225   Strains generated in this study, and the sequences of primers used for ChIP analysis are available

226   upon request. The Gene Expression Omnibus accession number for the ChIP-chip data reported

227   in this paper is GSE69642.

228

229   **RESULTS**

230   **Histone H3 N-terminal tails facilitate FACT interaction with chromatin *in vivo***

231   While Spt16 is enriched in coding regions of actively transcribing genes (MASON AND

232   STRUHL 2003; MAYER *et al.* 2010), the mechanisms by which it is recruited remains to be

233   established. Given that the FACT complex interacts with nucleosomes *in vitro*

234   (BELOTSERKOVSKAYA *et al.* 2003), it can be recruited through nucleosome interactions.

235   Moreover, Spt16 interaction was greatly reduced with the nucleosomes lacking the histone N-

236   terminal tails (NTTs) implicating histone tails in promoting Spt16-nucleosome interactions

237   (STUWE *et al.* 2008; VANDEMARK *et al.* 2008). Significantly, removal of the H3 and H4 tails, but

238   not of the H2A-H2B tails, abolished Spt16-histone interactions *in vitro* (WINKLER *et al.* 2011).

239   The H3 or H4 tails therefore could facilitate recruitment/retention of the FACT complex. To test

240   this possibility, we examined yeast Spt16 occupancy by ChIP in histone mutants lacking the H3

241   or H4 N-terminal tail. Spt16 occupancy in the *ARG1* 5' and 3' ORFs was reduced by ~50% in

242   the H3 mutants lacking 1-20 (*H3Δ1-20*) or 1-28 (*H3Δ1-28*) N-terminal residues (Figure 1A). In

243   comparison, in the H4 tail mutant (*H4Δ1-16*), only a small (~20%) reduction was observed in the

244   *ARG1* 3' ORF (Figure 1A). A substantial reduction in Spt16 occupancy (~80%) was also

245   observed at a constitutively expressed *ADH1* gene in the H3 mutants (Figure 1B), but not in the

246   H4 mutant (Figure S1A). Although, FACT/Spt16 interacts with both H3 and H4 tail peptides, *in*

247   *vitro,* (STUWE *et al.* 2008; VANDEMARK *et al.* 2008) it appears that the H3 tail may help in

248   recruiting or retaining FACT to its target genes, *in vivo*. Consistent with this idea, reduced

249   occupancy of Spt16 was also observed in the coding regions of *PYK1*, *PMA1* and *GLY1* genes

250   (Figure 1C). In contrast to the impaired Spt16 occupancy in the H3 mutant, for most genes, Pol II

251   occupancies were comparable in WT and the H3 mutants, except for the *GLY1* gene, which

252   showed a small reduction in Pol II occupancy (Figure S1B).

253   To further examine the role of the H3 tails in promoting FACT association with

254   chromatin, we performed coimmunoprecipitation assay. The HA-tagged histone H2B (H2B-HA)

255   efficiently pulled-down Spt16 from the whole cell extracts (WCEs) prepared from HA-tagged

256   WT cells but not from untagged cells (Figure 1D, left). We also observed a reduced Spt16 pull-

257   down from the *H3Δ1-28* WCEs (~50 %; Figure 1D, right). No such reduction in Spt16

258   occupancy was seen in the H4 tail deletion mutant (*H4Δ1-16*; Figure S1C), supporting the idea

259   that the H3 tail promotes Spt16 association with chromatin *in vivo*. However, the extent to which

260   the H3 tail contributes in this process may be variable, as observed by the differences of Spt16

261   occupancies at the different genes in the H3 mutant (Figure 1A-1C).

262

263   **Acetylation of the H3 tail promotes FACT occupancy at *ADH1* and *ARG1* genes**

264   After observing that the H3 tail contributes to Spt16, we examined the role for

265   posttranslational modifications on the H3 tail in regulating FACT localization to transcribed

266   genes. The H3 tail lysines, K4 and K36, are methylated by Set1 and Set2, respectively (BRIGGS

267   *et al.* 2001; STRAHL *et al.* 2002).To examine, whether the reduction in Spt16 occupancy in the

268   H3 tail deletion mutant is due to the loss of H3 methylation, we measured Spt16 enrichment in

269   the *set1Δ*/*set2Δ* double mutant. Comparable occupancies of Spt16 were observed in the ORFs of

270   *ARG1* and *ADH1* genes in WT and the *set1Δ*/*set2Δ* mutant (Figure 2A). Furthermore, we found

271   very similar signal for coimmunoprecipitation of Pol II with Spt16 in WT and *set1Δ/set2Δ* WCEs

272   (Figure 2B), suggesting that H3 methylation is likely dispensable for maintaining WT level of

273   FACT occupancy, at least, at these two genes. The H3 and H4 tails are also acetylated by Gcn5-

274   containing SAGA and Esa1-containing NuA4 histone acetyltransferase (HAT) complexes,

275   respectively. Accordingly, a *gcn5Δ/esa1ts* double mutant elicits strong reductions in H3 and H4

276   acetylation (GINSBURG *et al.* 2009). The *gcn5Δ/esa1ts* mutant, grown at the permissive

277   temperature 25°C (represented as *gcn5Δ*) or at the non-permissive temperature 37°C to inactivate

278   Esa1 (*gcn5Δ/esa1ts*), produced comparable reductions in Spt16 occupancy in the *ARG1* and

279   *ADH1* ORFs (Figure 2C and Figure S2B). In contrast, both WT and the HAT mutant displayed

280   comparable Pol II occupancies at *ARG1* and *ADH1* (Figure 2D, and Figure S2A). To examine

281   whether FACT occupancy correlates to H3 acetylation levels, we determined Spt16 enrichment

282   at *ARG1* in a histone deacetylase mutant, *rpd3Δ/hos2Δ*. Interestingly, Spt16 occupancy was not

283   reduced in the histone deacetylase mutant *rpd3Δ/hos2Δ* (Figure 2E). This is surprising given

284   that H3 acetylation levels were shown to be elevated in this mutant (GOVIND *et al.* 2010), and

285   that our current results reveal diminished FACT occupancy in the HAT mutant. It is possible that

286   the WT level of histone acetylation is sufficient for normal FACT occupancy, suggesting that

287   histone acetylation, but not deacetylation, plays a role in FACT recruitment/retention in coding

288   regions. As such, any further increase does not necessarily increase FACT occupancy. Taken

289   together, these results suggest a potential role for the acetylated H3 tail in promoting FACT

290   occupancy in the transcribed coding regions.

291   To provide additional proof for the role of histone acetylation, we examined Spt16

292   occupancy in the H3 and H4 tail point mutants. The H3 mutant (K4, K9, K14, K18 substituted to

293   alanine; H3K→A) displayed reduced Spt16 occupancy in the ORFs of both *ARG1* and *ADH1*

13

294   genes (Figure 2F). However, only minimal changes in Spt16 occupancy were observed in the H4

295   mutant (K5, K8, K12 and K16 substituted to arginine; H4K→R, or to glutamine H4K→Q)

296   (Figure 2G; H4K→A mutant exhibits a lethal phenotype). While Spt16 interacts with both H3

297   and H4 N-terminal tails, and the histone tail mutants impair FACT function (BISWAS *et al.* 2006;

298   VANDEMARK *et al.* 2008), our results suggest that acetylation of H3 tail makes a greater

299   contribution to the FACT occupancy in the coding regions.

300

301   **FACT and Spt6 are required for transcription genome-wide**

302   Microarray analyses examining transcription defects have revealed that the loss of Spt16

303   function leads to aberrant transcription at many genomic locations, including within coding

304   regions (CHEUNG *et al.* 2008; VAN BAKEL *et al.* 2013). While it is evident that Spt16 functions to

305   suppress wide-spread cryptic and anti-sense transcription, the role of FACT in regulating Pol II

306   occupancy in coding regions is not well understood at a genome-wide scale. Gene-specific

307   studies have suggested that FACT regulates transcription at the initiation step (BISWAS *et al.*

308   2006; JIMENO-GONZALEZ *et al.* 2006; DUINA *et al.* 2007). Additionally, FACT, in cooperation

309   with H2B ubiquitination, is important for restoration of chromatin in the wake of Pol II

310   elongation (FLEMING *et al.* 2008). As mentioned earlier, similar to the FACT complex, Spt6 (a

311   H3/H4 chaperone) is localized to the coding regions of strongly transcribed genes (MAYER *et al.*

312   2010; IVANOVSKA *et al.* 2011; PERALES *et al.* 2013; BURUGULA *et al.* 2014) and is also important

313   for suppressing aberrant transcription (KAPLAN *et al.* 2003; CHEUNG *et al.* 2008; VAN BAKEL *et*

314   *al.* 2013). To compare the impact of FACT and Spt6 on transcription, we utilized strains in

315   which the expression of *SPT16* or *SPT6* was under the control of a tetracycline repressible

14

316   promoter (*SPT16-TET* and *SPT6-TET*). These promoters can be repressed by growing cells in the

317   presence of doxycycline (dox).

318   To rule out unexpected consequences of replacing the endogenous promoter with the

319   TET-promoter, we first compared Spt16 and Spt6 protein levels in TET-strains and BY4741 (*S.*

320   *cerevisiae* WT strain). Spt16 and Spt6 protein levels in the untreated (no dox; ND) *SPT16-TET*

321   and *SPT6-TET*, respectively, were very similar to those detected in the BY4741 cells (Figure 3A,

322   top panel). As expected, treating *SPT16-TET* and *SPT6-TET* cells with dox led to reduced

323   expression of Spt16 and Spt6, respectively (Figure 3A, bottom panel). We noted that Spt16 was

324   depleted to a greater extent than Spt6 upon dox-treatment. Since Spt16 mutants have been shown

325   to cause cell cycle defects (PRENDERGAST *et al.* 1990), we also measured the level of budded and

326   unbudded cells in BY4741, *SPT16-TET* and *SPT6-TET* dox-treated cells. We did not find any

327   significant increase in the number of budded and unbudded cells under Spt6 or Spt16 depleted

328   conditions (Figure S3A), suggesting that depleting Spt16 or Spt6, under the experimental

329   conditions employed, elicit minimal cell cycle defects. Moreover, the TET-strains grown in the

330   presence or absence of dox, exhibited similar viability (Figure 3B). Altogether, these results

331   indicate that the untreated *SPT16-TET* and *SPT6-TET* cells behave similar to BY4741.

332   To examine the effects of depleting Spt16 and Spt6 on transcription, we determined Rpb3

333   occupancy in untreated cells (*SPT16-TET*; referred to as WT hereafter), and dox-treated *SPT16-*

334   *TET* (*spt16*) and *SPT6-TET* (*spt6*) cells by ChIP-chip. We observed a strong correlation (Pearson

335   correlation, r= 0.93) between the Pol II occupancies in the dox-untreated *SPT16-TET* and

336   BY4741 strains, genome-wide, which further indicated that replacing the endogenous *SPT16*

337   promoter with the TET-promoter does not adversely affect transcription. We also determined

338   Spt16 occupancy genome-wide by ChIP-chip and found that Spt16 occupancy in coding regions

15

339   strongly correlated with Pol II occupancy (Pearson correlation, r=0.85), in agreement with

340   previous studies (MAYER *et al.* 2010).

341   The heat-maps depicting changes in Rpb3 enrichment (*spt16*/WT) showed diminished

342   ratios in coding regions of the genes displaying the greatest Rpb3 enrichments in WT cells

343   (Figure 3C). Consistent with a strong correlation between Spt16 and Rpb3 occupancies, the

344   genes with the highest Spt16 enrichments showed greatest Rpb3 reductions (Figure 3D).

345   We also noted that deletion of Spt16 (and Spt6, described later) also revealed an increase

346   in Pol II occupancies at those genes, which otherwise show very poor enrichment ratios in WT

347   cells. Given that our ChIP-chip normalization was performed without spike-in control, this

348   apparent increase in Rpb3 occupancy is unlikely to be biologically relevant.

349   To further analyze the impact of depleting Spt16 on Pol II occupancy, we selected the top

350   25% genes showing greatest Rpb3 occupancy in WT cells (n=1246). Nearly identical profiles for

351   Rpb3 occupancy were observed in WT and BY4741 at the metagene comprised of these

352   transcribed genes (Figure 3E). However, Spt16 depletion evoked reduction in Pol II occupancy,

353   primarily in coding region of these sets of genes. Although reduced Pol II occupancy was

354   observed throughout the coding region, Pol II occupancy defect was more pronounced in the 5'

355   end. Intriguingly, Pol II occupancy appeared to increase towards the 3' end, relative to the 5'

356   end, in the Spt16-depleted cells. Considering that if Pol II fails to clear the promoter or

357   disengages near the 5' end under limited Spt16 availability, then Pol II occupancy should have

358   been low uniformly across coding region. The relative increase in Pol II occupancy towards the

359   3' end may reflect increased cryptic transcription events that accumulate Pol II from the 5' to 3'

360   end. Such an explanation would be consistent with the established role of histone chaperones in

361   suppressing cryptic transcription (KAPLAN *et al.* 2003; CHEUNG *et al.* 2008; VAN BAKEL *et al.*

16

362   2013). A previous study utilizing microarray predicted 960 and 1130 genes to have cryptic

363   transcription in *spt6-1004* and *spt16-197* mutants (CHEUNG *et al.* 2008). We found that only 154

364   genes, predicted to express cryptic transcripts in the previous study, were among the 1246 genes

365   exhibiting high-levels of Pol II occupancy (Figure S3B). Replotting Pol II occupancy data after

366   excluding these 154 genes (Figure S3C) displayed profiles similar to that observed in Figure 3E.

367   This analysis suggests that it is unlikely that differences in Pol II profiles observed under Spt6

368   and Spt16 depleted condition is a result of the presence of genes expected to display cryptic

369   transcription. It is possible that Pol II pausing and queuing Pol II in the 3' end superimposed on

370   elongation defects at the very 5' end could result in increased Pol II occupancy towards the 3'

371   end on depleting Spt16.

372   Given that Gcn4 target genes are activated under the growth conditions used (see

373   Materials and Methods), we additionally analyzed the effect of depleting Spt16 on transcription

374   of Gcn4 targets. 130 Gcn4-regulated genes were enriched among the top 1246 transcribed genes.

375   These genes also displayed a greater reduction in Pol II occupancy at the 5' end in Spt16-

376   depleted cells (Figure 3F). A similar profile for Rpb3 occupancy defect was observed in

377   ribosomal protein genes, which are among the highly transcribed genes (*data not shown*). We

378   identified 226 genes showing reduction in Pol II occupancy $\geq$0.5 $\log_2$ ratio (ChIP/input) in

379   Spt16-depleted cells (Figure 3G). Interestingly, these genes were enriched among the top 10%

380   transcribed genes (p-value=10^{-117}), suggesting that depletion of Spt16 imparts a significant effect

381   on Pol II occupancy at highly expressed genes. Collectively, these results show that Pol II

382   occupancy in coding region is differentially affected by the loss of Spt16 and implicates FACT

383   in regulating global transcription.

384   Next, we analyzed Pol II occupancy in the Spt6 depleted cells. Interestingly, at the top

385   25% of Pol II-occupied genes, Spt6-depletion elicited a greater reduction in Rpb3 occupancy

386   towards the 3' end (Figures 3C (right) and 3E), consistent with previous studies showing the

387   greatest Spt6 enrichments in the 3' ends of transcribed genes (PERALES *et al.* 2013; BURUGULA *et*

388   *al.* 2014). A 5' to 3' bias in Pol II occupancy was also evident at the Gcn4-targets (Figure 3F)

389   and at 238 genes, which showed a reduction in Pol II occupancy ≥ 0.5 $\log_2$ ratio (ChIP/input)

390   (Figure S3D). A progressive reduction in Pol II occupancy in the 5' to 3' direction, in Spt6-

391   depleted cells, suggests that Spt6 may regulate Pol II processivity. Alternately, given the role of

392   Spt6 activity in the 3'—mRNA processing, diminished Spt6 levels could also result in reduced

393   Pol II occupancy at the 3' end (KAPLAN *et al.* 2005). To distinguish between these two

394   possibilities, we analyzed Rpb3 occupancy at the top 25% transcribing genes based on their gene

395   length. All three groups of genes, long (> 2 kb), medium (1-2 kb) and short (0.5-1 kb), showed a

396   5' to 3' bias in Pol II occupancies (Figure 3H). Interestingly, however, long and medium genes

397   displayed a greater reduction in the 3' end compared to the short genes (0.5-1 kb) (Figure 3H and

398   S3E). A simpler explanation for this observation is that Spt6 promotes Pol II elongation, in

399   agreement with previous studies (ENDOH *et al.* 2004; ARDEHALI *et al.* 2009; PERALES *et al.*

400   2013). A 3—mRNA processing defect (KAPLAN *et al.* 2005) would be expected to produce

401   similar reductions in Pol II occupancies at the 3' end irrespective of gene length. Collectively,

402   our data suggest that loss of FACT and Spt6 functions produces distinct effects on Pol II

403   occupancy. However, the role of FACT and Spt6 in suppressing aberrant transcription, to some

404   extent, could have an effect on Pol II occupancy under depletion conditions.

405

406   **FACT and Spt6 differentially impacts transcription and histone occupancy**

18

407   To further address the functional overlap between FACT and Spt6, we examined genes,

408   which showed a reduction in Pol II occupancy ($\leq$ -0.5 $\log_2$ ratio) upon depleting these factors.

409   We found a significant overlap between the genes exhibiting Pol II fold-change $\log_2 \geq 0.5$ upon

410   depleting either Spt16 or Spt6 (p-value = 5.1 x 10^{-76}, n= 111) (Figure 4A). The genes showing

411   Pol II occupancy defects upon depleting either Spt16 or Spt6 (common; n=111) exhibited, on

412   average, higher Pol II occupancy (in WT cells) than those genes which showed defects only after

413   depleting either Spt16 or Spt6 (unique) (Figure 4B). This observation suggests that strongly

414   transcribed genes may need full functions of Spt6 and Spt16 for a high-level of transcription. It is

415   also interesting to note that while Spt6 depletion was less efficient compared to that of Spt16, it

416   nonetheless evoked very similar Pol II occupancy defects on these genes (Figure 4C). In contrast,

417   Rpb3 profiles at the genes uniquely affected by Spt6 or Spt16 depletion showed a distinct cohort

418   behavior. Greater reduction in Rpb3 occupancy was observed across the ORF of the Spt16-

419   unique genes (n=115) upon depletion of Spt16 than of Spt6 (Figure 4D). Unlike the 'common

420   genes' these genes tolerated a moderate loss of Spt6. Likewise, Spt6-unique genes (n=217)

421   displayed a stronger Pol II occupancy defect after depleting Spt6 than Spt16 (Figure 4E), which

422   was depleted to a larger extent. Considering that Spt6 exhibits higher occupancy towards the 3'

423   ends (MAYER *et al.* 2010; PERALES *et al.* 2013; BURUGULA *et al.* 2014), we analyzed

424   distribution of the gene-length in the three classes of genes. The longer genes were enriched in

425   the Spt6-unique and common genes, whereas Spt16-unique genes were shorter (Figure S4A and

426   S4B). Thus, it appears that the differential effect of Spt16 and Spt6 depletion could partly be due

427   to differences in their localization patterns over the coding sequences.

428   We further examined the differential effect of depletion by determining Rpb3 ChIP

429   occupancy at four genes, which showed comparable Spt6, and Spt16 occupancy in our ChIP-chip

19

430   experiments. Pol II occupancies in the ORFs of *GLY1*, *HAC1*, *BDF2*, and *PHM8* were

431   substantially reduced (~2-5 folds) upon Spt16 depletion (Figure 4F). By contrast, only a

432   moderate to negligible reduction was observed after depleting Spt6. For example, Rpb3 was

433   reduced by less than 1.5 folds at *GLY1*, *HAC1*, *PMH8* upon Spt6 depletion. Similarly, we found

434   that histone H3 occupancy was more severely reduced in 5' ORFs of these genes upon depleting

435   Spt16 than upon Spt6 (Figure 4G). Reduced H3 occupancies upon depletion of Spt16 and Spt6

436   are consistent with their role in histone reassembly. Bigger reductions in Pol II and H3

437   occupancies were not due to higher Spt16 occupancies at these genes compared to that of Spt6

438   (Figure 4H). Collectively, these results suggest that Spt6 and Spt16 may help promote

439   transcription in a gene-specific manner.

440

441   **Spt6 promotes histone eviction to promote transcription**

442   To further investigate whether Spt6 and FACT cooperate in promoting transcription, we

443   deleted the Spt6 tandem SH2 domain (tSH2; 202 residues from C-terminus), which mediates

444   Spt6 recruitment, genome-wide (MAYER *et al.* 2010; BURUGULA *et al.* 2014), in the *SPT16-TET*

445   background (*SPT16/spt6Δ202*). As expected, treating the *SPT16/spt6Δ202* mutant with dox

446   resulted in reduced Spt16 protein levels (Figure S5A). We then determined Rpb3 and H3

447   occupancies by ChIP-chip in untreated (*SPT16/spt6Δ202*) and dox-treated (*spt16/spt6Δ202*)

448   cells, and compared the occupancies with that of the untreated *SPT16-TET* cells (WT). The

449   changes in Rpb3 occupancy in untreated *SPT16/spt6Δ202* were significantly anti-correlated with

450   the Rpb3 occupancy in the WT cell (r= -0.81) (Figure 5A), indicating a strong requirement of

451   Spt6 in transcription, genome-wide. A modest but statistically significant reduction in Rpb3

452   occupancy was observed in dox-treated, *spt16/spt6Δ202,* cells compared to the untreated cells

453   (for the first decile, p =5.2 x 10^{-59}), indicating that these factors cooperate to promote efficient

454   transcription (Figure 5B).

455   Rpb3 profiles in *spt16/spt6Δ202* mutant revealed greatly diminished occupancy across

456   the coding regions of the top 25% Pol II-occupied genes (Figure S5B). We noted that untreated

457   *SPT16/spt6Δ202* elicited greater reduction in Pol II occupancy than observed upon depleting

458   Spt6 (compare Figures S5B and 3E). This could be a result of an incomplete depletion of Spt6,

459   and thus, enough Spt6 remains after dox-treatment to promote transcription, albeit at reduced

460   efficiency. It is also possible that the tSH2 domain has additional roles in modulating Spt6

461   function in a manner that deleting tSH2 evoked a stronger Pol II occupancy defect than depleting

462   Spt6. Nonetheless, these results indicate the importance of Spt6 in stimulating high-level

463   transcription, genome-wide. However, depleting Spt16 in *SPT16/spt6Δ202* cells produced only

464   modest reductions in Pol II occupancy at the top 25% Pol II occupied (Figure S5B). This

465   observation raises a possibility that FACT may require certain aspects of Spt6 function to

466   stimulate transcription. Such an explanation is consistent with the observation that Spt16

467   depletion elicited reduced Pol II occupancy in otherwise WT strain (Figures 3D-G).

468   To further address functional cooperation between Spt16 and Spt6, we focused on the

469   genes eliciting greater reduction in dox-treated *spt16/spt6Δ202* than in untreated cells. The top

470   200 genes showing the greatest Pol II occupancy defect revealed that depleting Spt16 in

471   *spt6Δ202* background significantly reduced Rpb3 occupancy across the coding region (Figure

472   5C). 137 of these 200 genes were among the top 25% expressed genes (n=1246) in WT cells.

473   While these 137 genes displayed greater Pol II occupancy defects in *SPT16/spt6Δ202* than

474   observed in Spt6 or Spt16 depleted cells, the greatest defect was observed in the double mutant

21

475   (Figure S5C). These observations suggest that FACT and Spt6 may act synergistically to

476   stimulate transcription of a subset of highly expressed genes.

477   We also examined the 63 lowly expressed genes among the 200 genes, which showed

478   greater reduction in the double mutant. While no significant reduction in Pol II occupancy was

479   seen either in *SPT16/spt6Δ202* mutant or in Spt6 and Spt16 depleted cells, occupancy was

480   significantly reduced in the double mutant (Figure 5D). This suggests that FACT may

481   redundantly act with Spt6 in promoting transcription of a subset of lowly expressed genes. More

482   sensitive methods may be needed to fully comprehend the extent to which Spt6 and FACT

483   coordinate transcription of lowly expressed genes, especially considering the technical

484   challenges in accurately measuring Pol II occupancies at genes expressed at very low levels.

485   We next examined histone occupancy changes in *spt16/spt6Δ202*. We found that the 137

486   highly expressed genes displayed increased histone occupancy across the metagene (Figure 5E).

487   The greatest increase in histone occupancy was observed slightly upstream of the TSS. Similar

488   profile was observed for the top 25% genes (n= 1246; data not shown). These results suggest that

489   in addition to reassembling histones, Spt6 may play a role in stimulating removal of histones

490   during transcription. Since histones pose a significant barrier to transcription (TEVES *et al.* 2014),

491   elevated histone occupancy could explain a robust transcription defect observed at transcribed

492   genes in *SPT16/spt6Δ202* cells. However, despite a greater reduction in Pol II occupancy in dox-

493   treated cells, no significant increase in H3 occupancy was observed in the double mutant

494   compared to the single. One possible explanation for these results is that FACT restructures

495   chromatin to enhance transcription in a manner independent of histone disassembly, as proposed

496   earlier (FORMOSA 2012). In contrast, the histone occupancy profile for the 67 genes (low

497   transcribed) was distinct from the highly expressed genes in that elevated histone occupancy near

498   the TSS was observed only in the *spt16/spt6Δ202* double mutant, but not in the single

499   (*SPT16/spt6Δ202*) (Figure 5F). However, in both treated and untreated cells, elevated histone

500   occupancies were observed downstream of the TSS. This observation is in agreement with the

501   Pol II occupancy defects, which were also observed only in the double mutant (Figure 5F).

502   Increased histone occupancies near the TSS and in coding regions are consistent with the idea

503   that histones pose a significant barrier to transcription and suggest a role for FACT and Spt6 in

504   modulating histone occupancy.

505

DISCUSSION

507   In this study, we have examined the role of two highly conserved histone chaperones,

508   Spt16 and Spt6, in regulating genome-wide transcription and histone occupancy, under amino

509   acid starvation conditions. Spt6 recruitment to coding regions is stimulated by the

510   phosphorylated Pol II CTD and by HDACs Rpd3 and Hos2 (MAYER *et al.* 2012; BURUGULA *et*

511   *al.* 2014). However, the mechanism by which the FACT complex associates with chromatin is

512   not well understood. Our results showing diminished occupancy of Spt16 at the ORFs of *ARG1*

513   and *ADH1* and reduced interaction with nucleosomes in mutants lacking the H3 tail (Figure 1A-

514   1C), suggests a role for the H3 tail in promoting FACT association with transcribed regions. Our

515   results additionally suggest that histone acetylation enhances the ability of the FACT complex to

516   associate with transcribed ORFs, since deleting Gcn5 (a H3 HAT) or mutating the H3 tail lysine

517   residues significantly dampened Spt16 enrichment in coding sequences of *ARG1* and *ADH1*

518   (Figures 2C and 2F). These results provide *in vivo* evidence for the previous studies showing

519   impaired FACT binding to the nucleosomes/histones lacking N-terminal tails (VANDEMARK *et*

520   *al.* 2008; WINKLER *et al.* 2011). Currently, however, which regions of Spt16 are required for

521   histone tail interactions is unclear. While Spt16 N-terminal domain of *S. pombe* was shown to be

522   important for interacting with H3 and H4 tails, in *S. cerevisiae*, this domain was found to be

523   dispensable (VANDEMARK *et al.* 2008).

524   Considering that Spt16 exhibits similar affinity towards the acetylated and unacetylated

525   histone peptides *in vitro* (STUWE *et al.* 2008), it is plausible that acetylation-mediated changes to

526   the nucleosome structure allow FACT to stably bind chromatin at transcribing loci. Consistent

527   with this idea, Gcn5 promotes histone eviction, Pol II elongation, and stimulates recruitment of

528   bromodomain-containing chromatin remodelers, RSC and SWI/SNF (GOVIND *et al.* 2007;

529   DUTTA *et al.* 2014; SPAIN *et al.* 2014). Additional contacts with core domains of H3/H4 and with

530   H2A/H2B through its C-terminal domain (WINKLER *et al.* 2011; KEMBLE *et al.* 2015) could

531   further stabilize FACT-chromatin interactions, thereby maintaining chromatin in an accessible

532   conformation to promote transcription, and concomitantly aiding in reassembly of evicted

533   histones in the wake of transcription (JAMAI *et al.* 2009). Additional factors may act

534   cooperatively with other factors to enhance FACT enrichment. For instance, FACT interacts with

535   the Paf1 complex, and chromatin remodeler Chd1, both of which are enriched in transcribed

536   regions (KROGAN *et al.* 2002; SQUAZZO *et al.* 2002; SIMIC *et al.* 2003).

537   Enrichment of FACT in coding regions (MAYER *et al.* 2010) (*data not shown*), and its

538   ability to promote Pol II transcription through the nucleosomal templates, *in vitro*,

539   (BELOTSERKOVSKAYA *et al.* 2003; HSIEH *et al.* 2013), strongly suggests a role for FACT in the

540   elongation step of transcription. FACT is linked to the reestablishment of the disrupted

541   chromatin structure in the wake of transcription (JAMAI *et al.* 2009), and consequently, in

542   suppressing aberrant transcription by preventing utilization of cryptic promoters (KAPLAN *et al.*

543   2003; CHEUNG *et al.* 2008; VAN BAKEL *et al.* 2013). Our data indicate that FACT is globally

544   required for promoting transcription in the coding regions. Spt16 deficiency reduced Pol II

545   occupancy in coding regions of highly transcribed genes, including of the ribosomal protein

546   genes and Gcn4 targets (Figure 3). It was previously reported that histone mutants which perturb

547   association of Spt16 (shift in occupancy towards the 3' end) also reduced Pol II occupancy at the

548   5' end of *PMA1* and *FBA1* genes (NGUYEN *et al.* 2013). Thus, it seems that impairing FACT

549   activity, through depletion of Spt16 or by altering FACT association in the coding region

550   (NGUYEN *et al.* 2013), elicit greater defects in transcription in the early transcribed regions.

551   These results raise a possibility that FACT may help polymerases in negotiating the nucleosomal

552   barrier downstream of the TSS. Such an idea is consistent with biochemical studies showing that

553   FACT relieves Pol II pauses well within the nucleosomes and acts primarily to overcome

554   tetramer-DNA contacts (BONDARENKO *et al.* 2006). Considering that the rate of elongation in the

555   early transcribed regions is slower than that observed in the mid or 3' end regions (DANKO *et al.*

556   2013), our findings suggest that FACT may help slow-moving polymerases to overcome the

557   nucleosomal barrier at the 5' ends of the transcribed genes. Although, nucleosomes are expected

558   to pose a similar block to elongating Pol II irrespective of their position along coding sequences,

559   nucleosomal impediment to transcription at the distal end may be additionally relieved by

560   factors, such as chromatin remodelers RSC and SWI/SNF, which are enriched in the ORFs of

561   many genes (DUTTA *et al.* 2014; SPAIN *et al.* 2014). Moreover, post-translational histone

562   modifications, which are not uniform across coding regions, may have a differential effect on the

563   FACT activity to stimulate transcription. In support of such a possibility, it was shown that the

564   FACT complex cooperates with H2B ubiquitination to regulate transcription both *in vitro* and *in*

565   *vivo* (PAVRI *et al.* 2006; FLEMING *et al.* 2008).

566   In contrast to FACT, Spt6-depletion diminished Pol II occupancy at the 3' end (Figures

567   3E-F and 3H). Lower Pol II occupancy towards the 3' end could result from a processivity defect

568   and/or from a specific defect at the 3' end. Our analyses, based on gene-length, favor the idea

569   that Spt6 enhances Pol II processivity, possibly through stimulating nucleosome eviction, or by

570   preventing premature dissociation during Pol II traversal through coding regions. Such an

571   interpretation is consistent with previous studies showing reduced Pol II occupancy at the 3' end

572   of exceptionally long-genes (PERALES *et al.* 2013). Spt6 has been also shown to enhance the rate

573   of Pol II elongation at heat-shock genes in *Drosophila* (ARDEHALI *et al.* 2009). Therefore,

574   reduced Pol II occupancy near the 3' ends of yeast genes suggests that Spt6 may function to help

575   elongating polymerase traverse coding regions through multiple mechanisms.

576   Pol II occupancy in the Spt6 mutant lacking the C-terminal tandem SH2 domain was

577   strongly correlated with Pol II occupancy in the WT cells, indicating a strong requirement for

578   Spt6 in stimulating transcription genome-wide. Even though depleting Spt16 in otherwise WT

579   cells evoked reduction in Pol II occupancy from highly transcribed genes, this surprisingly had

580   only a minor impact on Pol II occupancy at the majority of transcribed genes in *spt6Δ202* cells.

581   This suggests that both factors might have overlapping role and that FACT may rely on the

582   certain aspects of Spt6 functions in promoting transcription. It makes sense considering that

583   FACT, and Spt6 are recruited to transcribed regions (MAYER *et al.* 2010; BURUGULA *et al.*

584   2014), and that both factors can interact with H2A-H2B and H3-H4 (MCCULLOUGH *et al.* 2015).

585   Despite interacting with nucleosomes as well as with histones, unlike Spt6, FACT can reorganize

586   the nucleosome structure in a manner that increases DNA accessibility. This distinct ability of

587   FACT could explain reduction in Pol II occupancy observed in a subset of transcribed genes in

588   *spt16/spt6Δ202* double mutant, but not in the single mutant (Figure 5C).

589   The severe reduction in Pol II occupancy in *spt6Δ202* was associated with elevated

590   histone occupancy in both promoter and coding regions, implicating Spt6 in promoting histone

591   eviction to allow efficient transcription. Increased occupancy in the promoter regions observed in

592   the mutant, is in agreement with earlier studies showing that histones are evicted from promoters

593   to allow high-levels of transcription activity (REINKE *et al.* 2001; DION *et al.* 2007). Loss of Spt6

594   function in the ΔSH2 mutant could also be responsible for increased histone occupancies, in the

595   coding regions. This idea is supported by studies showing a role for Spt6 in enhancing elongation

596   rate (ARDEHALI *et al.* 2009) and promoting Pol II processivity ((PERALES *et al.* 2013) and Figure

597   3). However, considering that the Spt6 missing the tSH2 domain can still associate with the

598   ORFs albeit at a reduced level (MAYER *et al.* 2010; BURUGULA *et al.* 2014), it is plausible that

599   the ORF-associated mutant Spt6 acts in a non-specific manner and impairs transcription leading

600   to elevated histone occupancies across the coding regions. It is also possible that the tSH2

601   domain modulates Spt6 function such that Spt6 without this domain is impaired for its histone

602   eviction function, leading to strong transcription defects as observed in the *spt6Δ202* mutant.

603   The greater Pol II occupancy defect observed upon Spt16 depletion in the tSH2 mutant at a

604   subset of highly transcribed genes (137 genes, Figure S2C) could be explained by the property

605   of FACT to reorganize/destabilize histone-DNA interactions (XIN *et al.* 2009; FORMOSA 2012)

606   that allows Pol II to negotiate nucleosomal block without requiring eviction of histones.

607

ACKNOWLEDGEMENTS

612   (GM095514), and Center for Biomedical Research (CBR, Oakland University). We also

613   acknowledge the genomic core facility at Michigan State University.

614

615

616

617

618

619

620

621

622

623

624

625

626

627   **REFERENCES**

628   Andrulis, E. D., E. Guzman, P. Doring, J. Werner and J. T. Lis, 2000 High-resolution
629   localization of Drosophila Spt5 and Spt6 at heat shock genes in vivo: roles in promoter
630   proximal pausing and transcription elongation. Genes Dev 14**:** 2635-2649.
631   Ardehali, M. B., J. Yao, K. Adelman, N. J. Fuda, S. J. Petesch *et al.*, 2009 Spt6 enhances the
632   elongation rate of RNA polymerase II in vivo. EMBO J 28**:** 1067-1077.
633   Belotserkovskaya, R., S. Oh, V. A. Bondarenko, G. Orphanides, V. M. Studitsky *et al.*, 2003
634   FACT facilitates transcription-dependent nucleosome alteration. Science 301**:** 1090-
635   1093.
636   Billon, P., and J. Cote, 2013 Precise deposition of histone H2A.Z in chromatin for genome
637   expression and maintenance. Biochim Biophys Acta 1819**:** 290-302.
638   Biswas, D., R. Dutta-Biswas, D. Mitra, Y. Shibata, B. D. Strahl *et al.*, 2006 Opposing roles for
639   Set2 and yFACT in regulating TBP binding at promoters. EMBO Journal 25**:** 4479-4489.

640 Bondarenko, V. A., L. M. Steele, A. Ujvari, D. A. Gaykalova, O. I. Kulaeva *et al.*, 2006
641   Nucleosomes can form a polar barrier to transcript elongation by RNA polymerase II.
642   Mol Cell 24**:** 469-479.
643 Briggs, S. D., M. Bryk, B. D. Strahl, W. L. Cheung, J. K. Davie *et al.*, 2001 Histone H3 lysine 4
644   methylation is mediated by Set1 and required for cell growth and rDNA silencing in
645   Saccharomyces cerevisiae. Genes & Development 15**:** 3286-3295.
646 Brunelle, M., C. Coulombe, C. Poitras, M. A. Robert, A. N. Markovits *et al.*, 2015 Aggregate
647   and Heatmap Representations of Genome-Wide Localization Data Using VAP, a
648   Versatile Aggregate Profiler. Methods Mol Biol 1334**:** 273-298.
649 Burugula, B. B., C. Jeronimo, R. Pathak, J. W. Jones, F. Robert *et al.*, 2014 Histone deacetylases
650   and phosphorylated polymerase II C-terminal domain recruit Spt6 for cotranscriptional
651   histone reassembly. Mol Cell Biol 34**:** 4115-4129.
652 Cheung, V., G. Chua, N. N. Batada, C. R. Landry, S. W. Michnick *et al.*, 2008 Chromatin- and
653   Transcription-Related Factors Repress Transcription from within Coding Regions
654   throughout the Saccharomyces cerevisiae Genome. PLoS Biol 6**:** e277.
655 Close, D., S. J. Johnson, M. A. Sdano, S. M. McDonald, H. Robinson *et al.*, 2011 Crystal
656   structures of the S. cerevisiae Spt6 core and C-terminal tandem SH2 domain. J Mol Biol
657   408**:** 697-713.
658 Danko, C. G., N. Hah, X. Luo, A. L. Martins, L. Core *et al.*, 2013 Signaling pathways
659   differentially affect RNA polymerase II initiation, pausing, and elongation rate in cells.
660   Mol Cell 50**:** 212-222.
661 Dechassa, M. L., A. Sabri, S. Pondugula, S. R. Kassabov, N. Chatterjee *et al.*, 2010 SWI/SNF
662   has intrinsic nucleosome disassembly activity that is dependent on adjacent nucleosomes.
663   Mol Cell 38**:** 590-602.
664 Degennaro, C. M., B. H. Alver, S. Marguerat, E. Stepanova, C. P. Davis *et al.*, 2013 Spt6
665   regulates intragenic and antisense transcription, nucleosome positioning, and histone
666   modifications genome-wide in fission yeast. Mol Cell Biol 33**:** 4779-4792.
667 Dengl, S., A. Mayer, M. Sun and P. Cramer, 2009 Structure and in vivo requirement of the yeast
668   Spt6 SH2 domain. J Mol Biol 389**:** 211-225.
669 Dion, M. F., T. Kaplan, M. Kim, S. Buratowski, N. Friedman *et al.*, 2007 Dynamics of
670   Replication-Independent Histone Turnover in Budding Yeast. Science 315**:** 1405-1408.
671 Duina, A. A., A. Rufiange, J. Bracey, J. Hall, A. Nourani *et al.*, 2007 Evidence that the
672   Localization of the Elongation Factor Spt16 Across Transcribed Genes Is Dependent
673   Upon Histone H3 Integrity in Saccharomyces cerevisiae. Genetics 177**:** 101-112.
674 Dutta, A., M. Gogol, J.-H. Kim, M. Smolle, S. Venkatesh *et al.*, 2014 Swi/Snf dynamics on
675   stress-responsive genes is governed by competitive bromodomain interactions. Genes &
676   Development 28**:** 2314-2330.
677 Endoh, M., W. Zhu, J. Hasegawa, H. Watanabe, D. K. Kim *et al.*, 2004 Human Spt6 stimulates
678   transcription elongation by RNA polymerase II in vitro. Mol Cell Biol 24**:** 3324-3336.
679 Fleming, A. B., C.-F. Kao, C. Hillyer, M. Pikaart and M. A. Osley, 2008 H2B Ubiquitylation
680   Plays a Role in Nucleosome Dynamics during Transcription Elongation. Molecular Cell
681   31**:** 57-66.
682 Formosa, T., 2012 The role of FACT in making and breaking nucleosomes. Biochim Biophys
683   Acta 1819**:** 247-255.

684   Formosa, T., P. Eriksson, J. Wittmeyer, J. Ginn, Y. Yu *et al.*, 2001 Spt16-Pob3 and the HMG
685   protein Nhp6 combine to form the nucleosome-binding factor SPN. Embo j 20**:** 3506-
686   3517.
687   Ginsburg, D. S., C. K. Govind and A. G. Hinnebusch, 2009 NuA4 Lysine Acetyltransferase Esa1
688   Is Targeted to Coding Regions and Stimulates Transcription Elongation with Gcn5. Mol.
689   Cell. Biol. 29**:** 6473-6487.
690   Govind, C. K., D. Ginsburg and A. G. Hinnebusch, 2012 Measuring Dynamic Changes in
691   Histone Modifications and Nucleosome Density during Activated Transcription in
692   Budding Yeast. Methods Mol Biol 833**:** 15-27.
693   Govind, C. K., H. Qiu, D. S. Ginsburg, C. Ruan, K. Hofmeyer *et al.*, 2010 Phosphorylated Pol II
694   CTD recruits multiple HDACs, including Rpd3C(S), for methylation-dependent
695   deacetylation of ORF nucleosomes. Mol Cell 39**:** 234-246.
696   Govind, C. K., F. Zhang, H. Qiu, K. Hofmeyer and A. G. Hinnebusch, 2007 Gcn5 promotes
697   acetylation, eviction, and methylation of nucleosomes in transcribed coding regions. Mol
698   Cell 25**:** 31-42.
699   Gurard-Levin, Z. A., J. P. Quivy and G. Almouzni, 2014 Histone chaperones: assisting histone
700   traffic and nucleosome dynamics. Annu Rev Biochem 83**:** 487-517.
701   Hassan, A. H., K. E. Neely and J. L. Workman, 2001 Histone acetyltransferase complexes
702   stabilize swi/snf binding to promoter nucleosomes. Cell 104**:** 817-827.
703   Hondele, M., and A. G. Ladurner, 2011 The chaperone-histone partnership: for the greater good
704   of histone traffic and chromatin plasticity. Curr Opin Struct Biol 21**:** 698-708.
705   Hondele, M., T. Stuwe, M. Hassler, F. Halbach, A. Bowman *et al.*, 2013 Structural basis of
706   histone H2A-H2B recognition by the essential chaperone FACT. Nature 499**:** 111-114.
707   Hsieh, F. K., O. I. Kulaeva, S. S. Patel, P. N. Dyer, K. Luger *et al.*, 2013 Histone chaperone
708   FACT action during transcription through chromatin by RNA polymerase II. Proc Natl
709   Acad Sci U S A 110**:** 7654-7659.
710   Hughes, T. R., M. J. Marton, A. R. Jones, C. J. Roberts, R. Stoughton *et al.*, 2000 Functional
711   discovery via a compendium of expression profiles. Cell 102**:** 109-126.
712   Ivanovska, I., P. E. Jacques, O. J. Rando, F. Robert and F. Winston, 2011 Control of chromatin
713   structure by spt6: different consequences in coding and regulatory regions. Mol Cell Biol
714   31**:** 531-541.
715   Jamai, A., A. Puglisi and M. Strubin, 2009 Histone Chaperone Spt16 Promotes Redeposition of
716   the Original H3-H4 Histones Evicted by Elongating RNA Polymerase. Molecular Cell
717   35**:** 377-383.
718   Jeronimo, C., S. Watanabe, C. D. Kaplan, C. L. Peterson and F. Robert, 2015 The Histone
719   Chaperones FACT and Spt6 Restrict H2A.Z from Intragenic Locations. Mol Cell 58**:**
720   1113-1123.
721   Jimeno-Gonzalez, S., F. Gomez-Herreros, P. M. Alepuz and S. Chavez, 2006 A gene-specific
722   requirement for FACT during transcription is related to the chromatin organization of the
723   transcribed region. Mol Cell Biol 26**:** 8710-8721.
724   Kaplan, C. D., M. J. Holland and F. Winston, 2005 Interaction between transcription elongation
725   factors and mRNA 3'-end formation at the Saccharomyces cerevisiae GAL10-GAL7
726   locus. J Biol Chem 280**:** 913-922.
727   Kaplan, C. D., L. Laprade and F. Winston, 2003 Transcription elongation factors repress
728   transcription initiation from cryptic sites. Science 301**:** 1096-1099.

729   Kaplan, C. D., J. R. Morris, C. Wu and F. Winston, 2000 Spt5 and spt6 are associated with active
730   transcription and have characteristics of general elongation factors in D. melanogaster.
731   Genes Dev 14: 2623-2634.
732   Kato, H., K. Okazaki, T. Iida, J. Nakayama, Y. Murakami et al., 2013 Spt6 prevents
733   transcription-coupled loss of posttranslationally modified histone H3. Sci Rep 3.
734   Kemble, D. J., L. L. McCullough, F. G. Whitby, T. Formosa and C. P. Hill, 2015 FACT Disrupts
735   Nucleosome Structure by Binding H2A-H2B with Conserved Peptide Motifs. Mol Cell
736   60: 294-306.
737   Kireeva, M. L., W. Walter, V. Tchernajenko, V. Bondarenko, M. Kashlev et al., 2002
738   Nucleosome remodeling induced by RNA polymerase II: loss of the H2A/H2B dimer
739   during transcription. Mol Cell 9: 541-552.
740   Krogan, N. J., M. Kim, S. H. Ahn, G. Zhong, M. S. Kobor et al., 2002 RNA polymerase II
741   elongation factors of Saccharomyces cerevisiae: a targeted proteomics approach. Mol
742   Cell Biol 22: 6979-6992.
743   Lee, C.-K., Y. Shibata, B. Rao, B. D. Strahl and J. D. Lieb, 2004 Evidence for nucleosome
744   depletion at active regulatory regions genome-wide. Nat Genet 36: 900-905.
745   Li, B., M. Carey and J. L. Workman, 2007 The role of chromatin during transcription. Cell 128:
746   707-719.
747   Liu, J., J. Zhang, Q. Gong, P. Xiong, H. Huang et al., 2011 Solution structure of tandem SH2
748   domains from Spt6 protein and their binding to the phosphorylated RNA polymerase II
749   C-terminal domain. J Biol Chem 286: 29218-29226.
750   Mason, P. B., and K. Struhl, 2003 The FACT complex travels with elongating RNA polymerase
751   II and is important for the fidelity of transcriptional initiation in vivo. Mol Cell Biol 23:
752   8323-8333.
753   Mayer, A., M. Heidemann, M. Lidschreiber, A. Schreieck, M. Sun et al., 2012 CTD tyrosine
754   phosphorylation impairs termination factor recruitment to RNA polymerase II. Science
755   336: 1723-1725.
756   Mayer, A., M. Lidschreiber, M. Siebert, K. Leike, J. Soding et al., 2010 Uniform transitions of
757   the general RNA polymerase II transcription complex. Nat Struct Mol Biol 17: 1272-
758   1278.
759   McCullough, L., Z. Connell, C. Petersen and T. Formosa, 2015 The Abundant Histone
760   Chaperones Spt6 and FACT Collaborate to Assemble, Inspect, and Maintain Chromatin
761   Structure in Saccharomyces cerevisiae. Genetics 201: 1031-1045.
762   Mnaimneh, S., A. P. Davierwala, J. Haynes, J. Moffat, W. T. Peng et al., 2004 Exploration of
763   essential gene functions via titratable promoter alleles. Cell 118: 31-44.
764   Nguyen, H. T., W. Wharton, 2nd, J. A. Harper, J. R. Dornhoffer and A. A. Duina, 2013 A
765   nucleosomal region important for ensuring proper interactions between the transcription
766   elongation factor Spt16 and transcribed genes in Saccharomyces cerevisiae. G3
767   (Bethesda) 3: 929-940.
768   Pavri, R., B. Zhu, G. Li, P. Trojer, S. Mandal et al., 2006 Histone H2B monoubiquitination
769   functions cooperatively with FACT to regulate elongation by RNA polymerase II. Cell
770   125: 703-717.
771   Perales, R., B. Erickson, L. Zhang, H. Kim, E. Valiquett et al., 2013 Gene promoters dictate
772   histone occupancy within genes. EMBO J 32: 2645-2656.

773 Prendergast, J. A., L. E. Murray, A. Rowley, D. R. Carruthers, R. A. Singer *et al.*, 1990 Size
774   selection identifies new genes that regulate Saccharomyces cerevisiae cell proliferation.
775   Genetics 124**:** 81-90.
776 Ransom, M., S. K. Williams, M. L. Dechassa, C. Das, J. Linger *et al.*, 2009 FACT and the
777   proteasome promote promoter chromatin disassembly and transcriptional initiation. J Biol
778   Chem 284**:** 23461-23471.
779 Reinke, H., P. D. Gregory and W. Horz, 2001 A Transient Histone Hyperacetylation Signal
780   Marks Nucleosomes for Remodeling at the *PHO8* Promoter in Vivo. Mol.Cell. 7**:** 529-
781   538.
782 Simic, R., D. L. Lindstrom, H. G. Tran, K. L. Roinick, P. J. Costa *et al.*, 2003 Chromatin
783   remodeling protein Chd1 interacts with transcription elongation factors and localizes to
784   transcribed genes. Embo J 22**:** 1846-1856.
785 Spain, M. M., S. A. Ansari, R. Pathak, M. J. Palumbo, R. H. Morse *et al.*, 2014 The RSC
786   complex localizes to coding sequences to regulate Pol II and histone occupancy. Mol Cell
787   56**:** 653-666.
788 Squazzo, S. L., P. J. Costa, D. L. Lindstrom, K. E. Kumer, R. Simic *et al.*, 2002 The Paf1
789   complex physically and functionally associates with transcription elongation factors in
790   vivo. EMBO J 21**:** 1764-1774.
791 Strahl, B. D., P. A. Grant, S. D. Briggs, Z. W. Sun, J. R. Bone *et al.*, 2002 Set2 is a nucleosomal
792   histone H3-selective methyltransferase that mediates transcriptional repression. Mol Cell
793   Biol 22**:** 1298-1306.
794 Stuwe, T., M. Hothorn, E. Lejeune, V. Rybin, M. Bortfeld *et al.*, 2008 The FACT Spt16
795   "peptidase" domain is a histone H3-H4 binding module. Proc Natl Acad Sci U S A 105**:**
796   8884-8889.
797 Takahata, S., Y. Yu and D. J. Stillman, 2009 FACT and Asf1 Regulate Nucleosome Dynamics
798   and Coactivator Binding at the HO Promoter. Molecular Cell 34**:** 405-415.
799 Teves, S. S., C. M. Weber and S. Henikoff, 2014 Transcribing through the nucleosome. Trends
800   Biochem Sci 39**:** 577-586.
801 van Bakel, H., K. Tsui, M. Gebbia, S. Mnaimneh, T. R. Hughes *et al.*, 2013 A Compendium of
802   Nucleosome and Transcript Profiles Reveals Determinants of Chromatin Architecture
803   and Transcription. PLoS Genet 9**:** e1003479.
804 VanDemark, A. P., H. Xin, L. McCullough, R. Rawlins, S. Bentley *et al.*, 2008 Structural and
805   functional analysis of the Spt16p N-terminal domain reveals overlapping roles of yFACT
806   subunits. J Biol Chem 283**:** 5058-5068.
807 Venkatesh, S., M. Smolle, H. Li, M. M. Gogol, M. Saint *et al.*, 2012 Set2 methylation of histone
808   H3 lysine 36 suppresses histone exchange on transcribed genes. Nature 489**:** 452-455.
809 Winkler, D. D., U. M. Muthurajan, A. R. Hieb and K. Luger, 2011 Histone chaperone FACT
810   coordinates nucleosome interaction through multiple synergistic binding events. J Biol
811   Chem 286**:** 41883-41892.
812 Xin, H., S. Takahata, M. Blanksma, L. McCullough, D. J. Stillman *et al.*, 2009 yFACT Induces
813   Global Accessibility of Nucleosomal DNA without H2A-H2B Displacement. Molecular
814   Cell 35**:** 365-376.

815

816

817

818

819

820

821

822

823

824

825

826

827

828

829

830

831

832

833

834

835

836

837

838   **Legends to the Figures:**

839   **Figure 1: The H3 N-terminal tail promotes FACT recruitment.**

840   A-B) ChIP occupancy of Myc-tagged Spt16 in WT and mutants lacking the H3 N-terminal tail
841   residues 1-20 (*H3Δ1-20*) or 1-28 (*H3Δ1-28*) and 1-16 residues of H4 (*H4Δ1-16*) at *ARG1* (A)
842   and in H3 mutants at *ADH1* (B). Graphs show mean and SEM. * represents a p-value < 0.01, **
843   represents a p-value < 0.001, and *** represents a p-vlaue <0.0001.

844   C) ChIP occupancies of Myc-tagged Spt16 at the indicated genes in the WT and the H3 tail
845   mutant, *H3Δ1-28*. * represents a p-value < 0.01, ** represents a p-value < 0.001.

33

846 D) Whole-cell extracts prepared from HA-tagged H2B WT and *H3Δ1-28* strains were pulled-
847 down with the anti-HA beads, and the immunoprecipitates were subjected to western blot using
848 antibodies against Spt16 and HA. Untagged WT was used as a control. The representative blot is
849 shown on the left, and the quantified data on the right.

850

851 **Figure 2: Role of the acetylated H3 tail in modulating Spt16 occupancy .**

852 A) ChIP enrichment of Spt16-Myc at *ARG1* in WT and histone methyltransferase mutant
853 *set1Δ/set2Δ*. * represents a p-value < 0.001, and ** represents a p-vlaue <0.0001.

854 B) Whole-cell extracts prepared from Spt16-Myc tagged WT and *set1Δ/set2Δ* strains were
855 immunoprecipitated with anti-Myc antibodies, and the immunoprecipitates were analyzed by
856 western blot to detect signals for Myc and Rpb3. Untagged WT was used as a control. Rpb3
857 band in immunoprecipitated samples is shown by an arrow and the IgG heavy chain by an
858 asterisk (*).

859 C) Spt16-Myc ChIP occupancy in WT and *gcn5Δ/esa1* histone acetyletransferase (HAT)
860 mutant. Spt16-Myc occupancies were measured by ChIP at *ARG1* and *ADH1* in a *gcn5Δ/esa1ts*
861 strain grown either at 25°C (represented as *gcn5Δ*) or at 37°C to inactivate Esa1 (*gcn5Δ/esa1*).
862 Graphs show mean and SEM. * represents a p-value < 0.001, and ** represents a p-vlaue
863 <0.0001. Spt16 occupancy differences between *gcn5Δ* and *gcn5Δ/esa1ts* were not significnat
864 (N.S).

865 D) Rpb3 occupancies in WT and *gcn5Δ/esa1ts* at *ARG1* and *ADH1*.

866 E) Spt16 occupancies in WT and HDAC mutant *hos2Δ/rpd3Δ* at *ARG1*.

867 F-G) Spt16-Myc enrichments at *ARG1* and at *ADH1* in histone H3 (F) and H4 tail mutants (G).
868 H3 K4, K9, K14, K18 substituted to alanine, H3K→A; H4 K5, K8, K12 and K16 substituted to
869 arginine; H4K→R, or to glutamine H4K→Q. Graphs show mean and SEM. ** represents a p-
870 vlaue <0.0001.

871

872 **Figure 3: Effect of depleting Spt16 and Spt6 on Pol II occupancy genome-wide.**

873 A) *BY4741*, *SPT16-TET* and *SPT6-TET* cells were grown in SC media and induced by SM.
874 Western blots show Spt16 and Spt6 protein levels in BY4741, *SPT16-TET* and *SPT6-TET* strains
875 without dox-treatment (top panel). The Spt16 and Spt6 levels in untreated (ND) and dox-treated
876 TET-strains are shown (bottom panel).

877 B) *SPT16-TET* and *SPT6-TET* cells grown and subcultured in SC media, with and without
878 doxycycline (dox), were collected, serially 10-fold diluted, and spotted on SC plates. Growth for
879 the two cultures of each *SPT16-TET* (left) and *SPT6-TET* (right) with and without dox (no-dox)
880 treatment are shown.

881   C) Heat-maps depicting genome-wide Rpb3 (Pol II) enrichment in *SPT16-TET* (without dox;
882   WT) (left), and changes in Rpb3 occupancies in dox-treated *SPT16-TET* (*spt16*/WT) (middle)
883   and *SPT6-TET* (*spt6*/WT) (right). Genes were sorted from highest to lowest ORF Rpb3
884   enrichment in WT cells.

885   D) Box-plot showing the changes in Rpb3 occupancy according to the Spt16 enrichment in
886   deciles. The average ORF occupancy of Rpb3 in *SPT16-TET* dox-treated and untreated cells was
887   determined, and the change in Rpb3 occupancy on depleting Spt16 (dox/no dox) was calculated
888   for each gene. Genes were then grouped into deciles according to the Spt16 occupancy in WT
889   cells. The first decile shows the highest Spt16 occupancy and the 10th shows the lowest.

890   E) Rpb3 occupancy profiles for the top 25% Pol II-occupied genes (n=1246) in untreated
891   *BY4741* and *SPT16-TET* (WT), and in dox-treated *SPT16-TET* (*spt16*) and *SPT6-TET* (*spt6*) cells
892   are shown.

893   F) Rpb3 occupancy profiles in untreated *SPT16-TET* (WT), and dox-treated *SPT16-TET* (*spt16*)
894   and *SPT6-TET* (*spt6*) cells at the Gcn4 targets genes enriched in the top 25% Pol II-occupied
895   genes.

896   G) Rpb3 occupancy profile at the genes eliciting reduction in Rpb3 occupancy ≥ 0.5 $\log_2$ ratio
897   (ChIP/input) on depleting Spt16 in WT and *spt16*.

898   H) The top 25% Pol II-occupied genes were grouped on the basis of their gene-length and Rpb3
899   occupancy profiles for the long (>2 kb), medium (1-2 kb), and short (0.5-1 kb) are shown in the
900   WT and Spt6-depleted cells.

901

902   **Figure 4: FACT promotes nucleosome reassembly.**

903   A) Venn diagram showing overlap among the genes which displayed Rpb3 occupancy defect
904   >0.5 $\log_2$ ratio (ChIP/Input) in Spt16 and Spt6 depleted cells. p-value for the overlap is shown.

905   B) Box-plot showing Rpb3 average ChIP-chip enrichments at Spt16-unique, Spt6-unique, and
906   Spt16 and Spt6 common genes in WT, Spt16-depleted and Spt6-depleted cells.

907   C-E) Metagene analysis for changes in Pol II enrichment under Spt16 and Spt6 depeleted cells,
908   for genes showing reduction > 0.5 $\log_2$ ratio (ChIP/Input) under Spt16 or Spt6 depleted condition
909   (C; common), only under Spt16 depletion (D) only under Spt6 depletion (E).

910   F-H) ChIP occupancies of Rpb3 (F), histone H3 (G), and of Spt6 and Spt16 in 5' ORFs of
911   indicated genes in *SPT16-TET* and *SPT6-TET* untreated (ND) or dox-treated (dox) cells. *
912   represents a p-value < 0.05, and ** represents a p-vlaue <0.001.

913

914   **Figure 5: Spt6 promotes histone eviction and transcription.**

A) The changes in Rpb3 occupancies (log$_2$ ratio, ChIP/input) in the untreated (no dox) and treated (dox) *spt16/spt6Δ202* cells relative to occupancies in the untreated *SPT16-TET* (WT) are plotted against the Rpb3 ORF occupancies in WT. Pearson correlations are shown.

B) Box-plot showing changes in Rpb3 occupancy in *SPT16/spt6Δ202* (dox and no dox) relative to the *SPT16-TET* (no dox) WT cells, at the genes grouped in deciles on the basis of the average ORF Rpb3 occupancies observed in WT cells. The first decile shows the highest Rpb3 occupancy and the 10th shows the lowest.

C) Top 200 genes showing the greatest reduction in Pol II occupancy in dox-treated *SPT16/spt6Δ202* relative to the untreated cells were selected based on the averge Rpb3 enrichments in coding regions. Pol II occupancy profile for these genes is plotted for WT, *SPT16/spt6Δ202* and *spt16/spt6Δ202*.

D) Box-plot showing average Rpb3 enrichment (log$_2$ ratio, ChIP/input) for 67 genes of the 200 genes. These genes were not among the top 25% genes showing greatest Rpb3 enrichment in WT cells. p-values are shown.

E-F) H3 occupancy profile for 137 highly expressed genes (E) and at 67 lowly expressed genes among the 200 genes showing greatest reduction in *Spt16/spt6Δ202* dox-treated compared to untreated cells (F).

Legends to the supplemental figures:

Figure S1: Role of the H3 tail in FACT recruitment.

A) Spt16 ChIP occupancy at *ADH1* in a H4 tail mutant lacking the first 16 residues (*H4Δ1-16*).

B) Spt16 and Rpb3 ChIP occupancy in the mutant was normalized against the WT occupancy at each gene and the normalized data is presented for the indicated genes.

C) Anti-HA beads were used to pull down HA-tagged H2B from the whole cell extracts prepared from the untagged WT, the HA-tagged WT and *H4Δ1-16* cells. The immunoprecipitates were subjected to western blot using anti-HA and anti-Spt16 antibodies. The representative blot is shown on the left, and the quantified data on the right.

Figure S2: Role of histone acetylation in recruiting Spt16.

ChIP occupancies of Rpb3 (left) and Spt16 (right) at *ARG1* in WT, *H3K→A,* and *gcn5Δ* mutants were determined by real-time (RT) PCR. ChIP occupancy in the *ARG1* 3' ORF in WT were normalized to *POL1* signals from the same ChIP sample, and normalized again with the *ARG1/POL1* signals for the related input samples. Average data with SEM for three independent experiments is shown.

951

Figure S3: Rpb3 occupancy in WT, and Spt16 and Spt6 depleted cells.

A) A bar-graph showing the bud counts in *SPT16-TET* and *SPT6-TET* cells in the presence or in the absence of doxycycline (dox). The cells were grown exactly as they were for the ChIP-chip experiments. The cells were briefly sonicated before counting budded and unbudded cells under the microscope. The error bars represent standard error of the mean.

B) Venn diagram showing overlap between the top 25% Pol II-occupied genes and those genes which were identified to express cryptic transcripts in *spt16-197* and *spt6-1004* (Cheung et al. 2008).

C) Overlapping genes, identified to express cryptic transcripts and were among the top 25% Pol II occupied genes (n=154), were removed from the list of 1246 highly expressed genes. Pol II occupancy profile for the remaining 1092 genes in WT, spt16 and spt6 cells is shown.

D) Rpb3 occupancy profile of WT and *spt6* cells at the genes eliciting reduction in Rpb3 occupancy ≥ 0.5 $\log_2$ ratio (ChIP/input) upon depleting Spt6.

E) The top 25% Pol II-occupied genes were grouped on the basis of their gene-length and changes in Rpb3 occupancy profiles (*spt6*/WT) for the long (>2 kb), medium (1-2 kb), and short (0.5-1 kb) are shown in the WT and Spt6-depleted cells.

968

Figure S4: Gene-length analyses for the genes most affected by depletion of Spt6 or Spt16.

A) The genes which showed more than 0.5 $\log_2$ reduction in Pol II occupancy upon depleting either Spt6 or Spt16 were analyzed, and were classified as Spt16-unique, Spt6-unique and Spt16-Spt6-common depending on whether they were enriched only upon depleting Spt16, Spt6 or both, respectively. Frequency distribution of these classes of genes based on their gene-length is plotted as a histogram.

B) Gene-length for the three classes of genes is shown in the box plot. Center lines show the medians; box limits indicate the 25th and 75th percentiles as determined by R software; whiskers extend 1.5 times the interquartile range from the 25th and 75th percentiles, outliers are represented by dots. 115, 217 and 111 genes were present in the Spt16-unique, Spt6-unique and common gene-sets, respectively.

980

**Figure S5: Pol II occupancy in *spt16/spt6Δ202* cells.**

A) Western blot showing Spt16 protein levels in untreated and dox-treated *Spt16/spt6Δ202* cells.

B) Rpb3 occupancy profiles for the top 25% Pol II-occupied genes (n=1246) in untreated *SPT16/spt6Δ202* and dox-treated (*spt16/spt6Δ202*) cells.

C) Box-plot showing Rpb3 enrichment ($\log_2$ ratio, ChIP/input) for the 137 highly expressed genes among the 200 genes showing greatest reduction in *Spt16/spt6Δ202* dox-treated compared

37

987   to untreated cells. Pol II occupancies are shown for the untreated WT and *SPT16/spt6Δ202*, and
988   dox-treated *SPT16-TET* (*spt16*) and *SPT6-TET* (*spt6*) and *SPT16/spt6Δ202* (*spt16/spt6Δ202*)
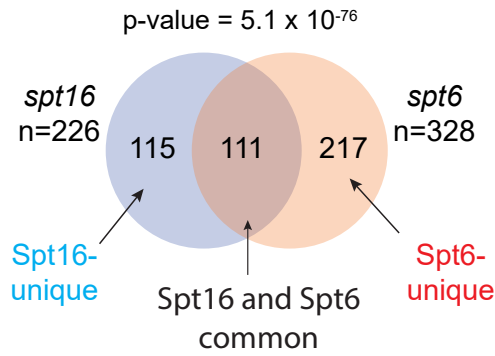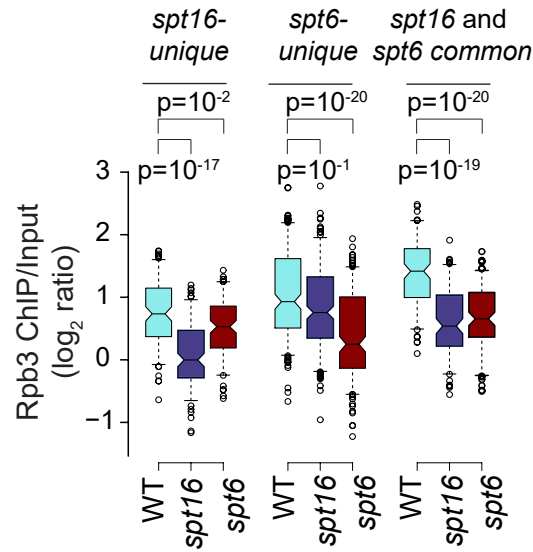989   cells.

Pathak_Figure 1
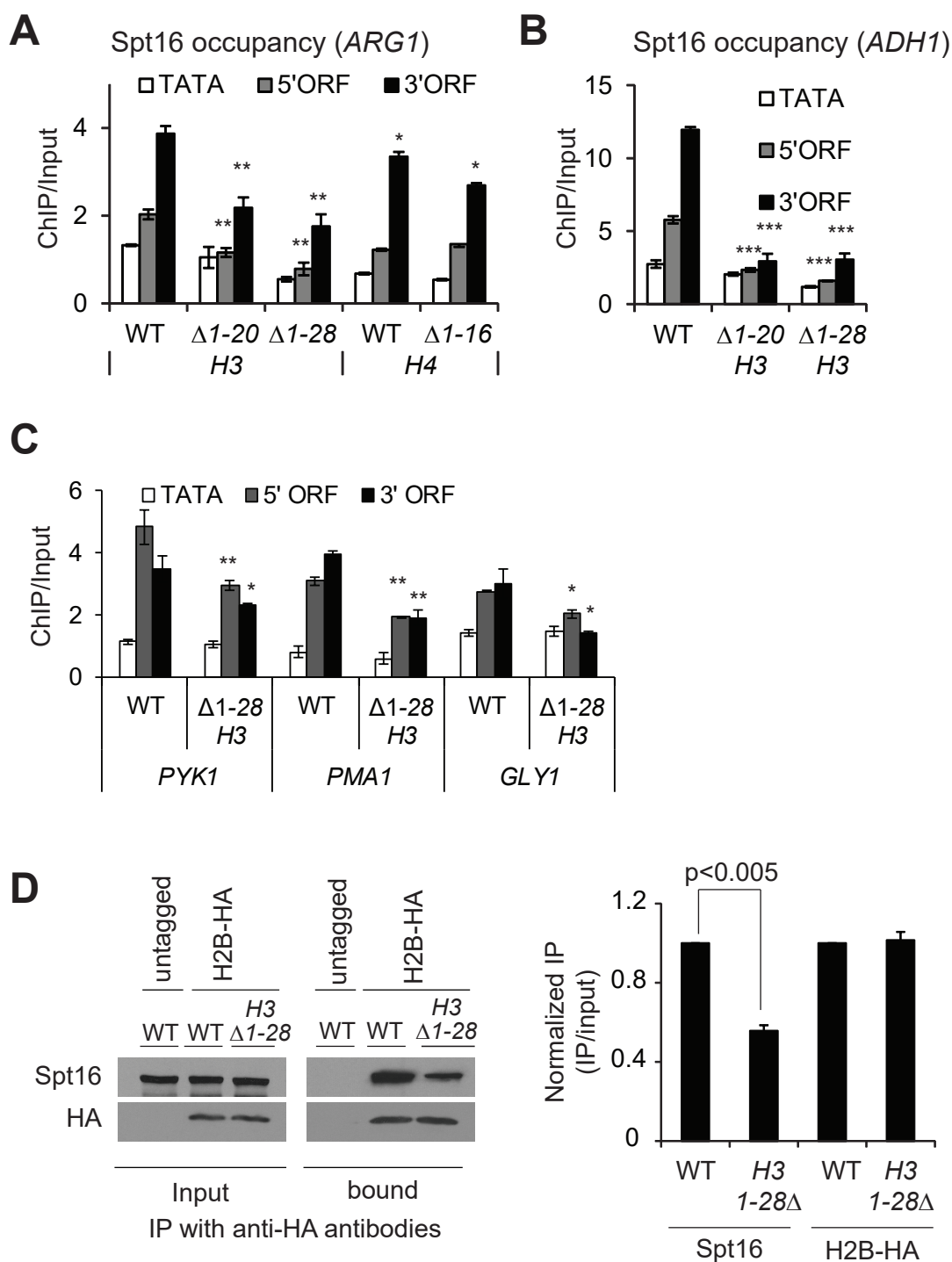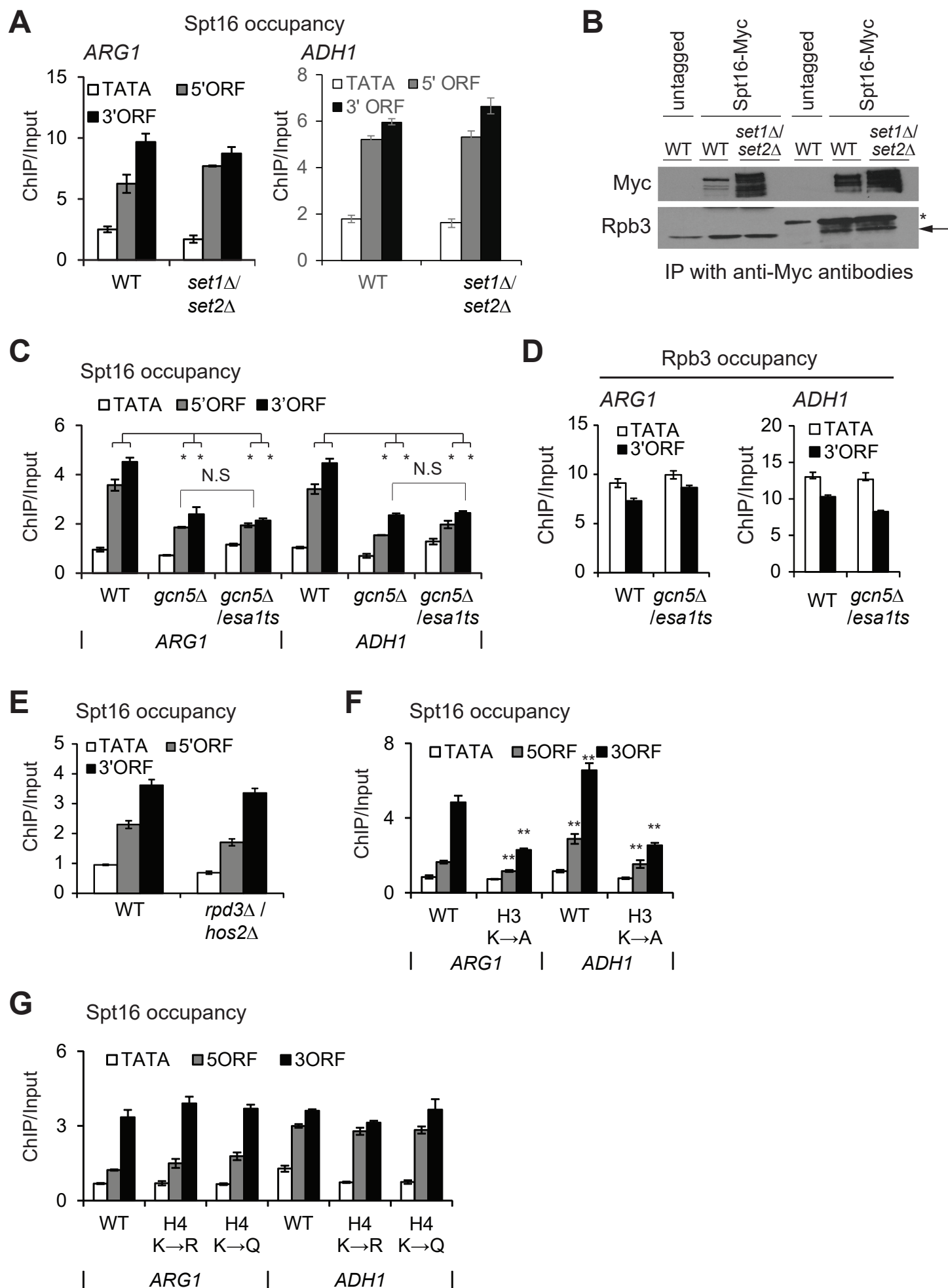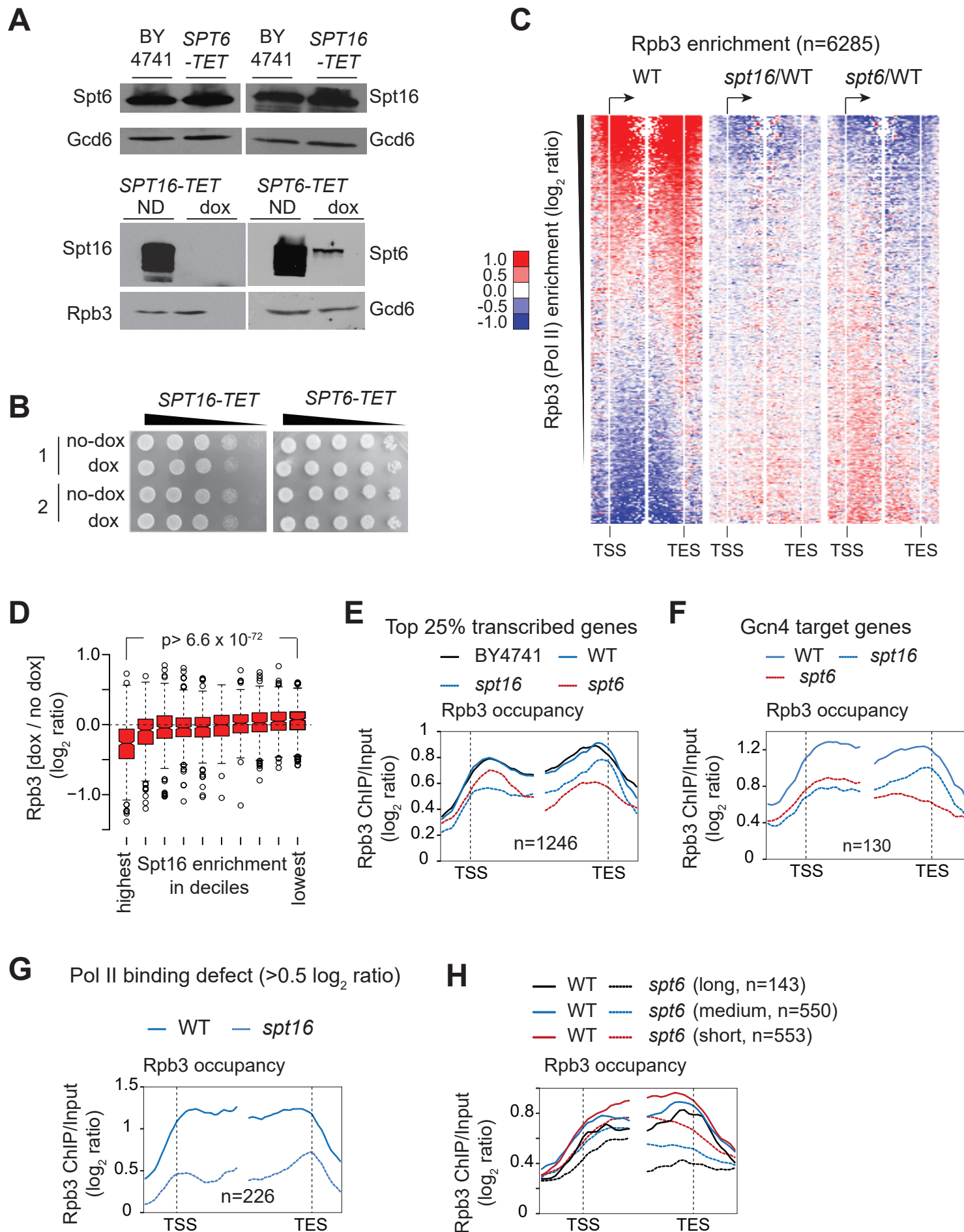
A Genes with reduced Pol II occupancy $\log_2$ (mutant / WT) $\leq$ -0.5
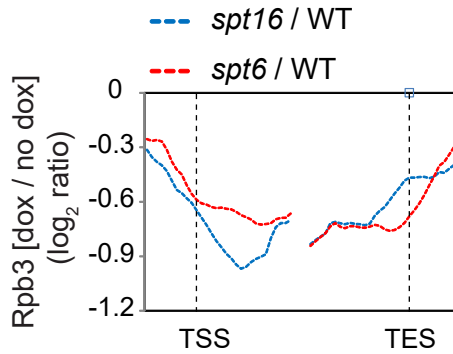
B Genes with reduced Pol II occupancy $\leq$ -0.5 in
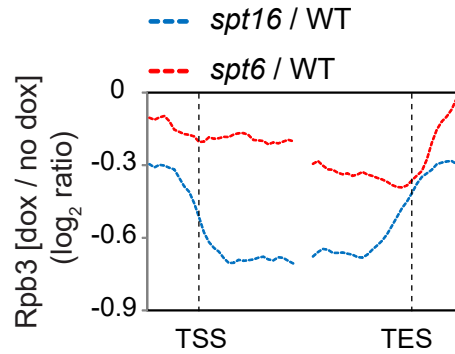
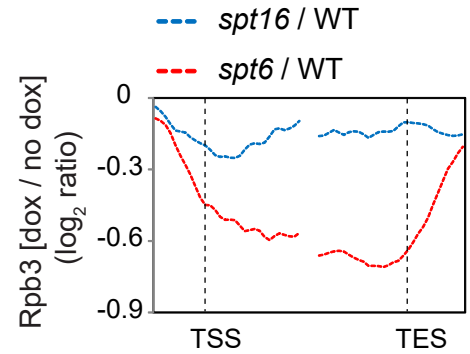**C** Genes with reduced Pol II occupancy $\leq$ -0.5 in both *spt16 and spt6* cells

D Genes with reduced Pol II occupancy $\leq$ -0.5 only in *spt16* cells
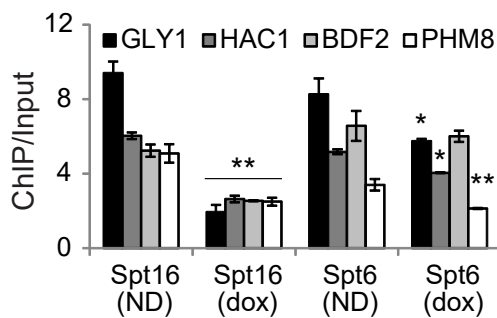
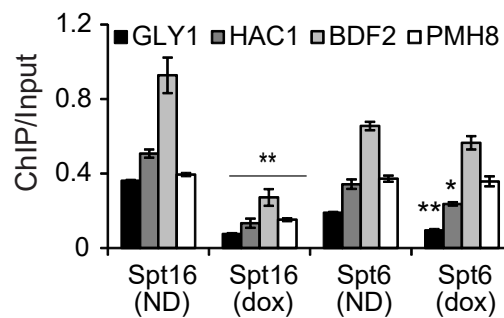**E** Genes with reduced Pol II occupancy $\leq$ -0.5 only in *spt6* cells

F Rpb3 occupancy

G H3 occupancy

H Spt16 and Spt6 occupancy

A All genes (n = 6246)

- *SPT16/spt6Δ202* (no dox)
- *spt16/spt6Δ202* (dox)

r= -0.82
r= -0.81

Changes in Rpb3 occupancy (ChIP/input) [*spt16/spt6Δ202 / WT*] (log$_2$ ratio)

Rpb3 enrichment in WT (log$_2$ ratio)

B *SPT16 / spt6Δ202*

no dox   dox

p = 5.2 x 10^{-59}

Changes in Rpb3 occupancy (ChIP/input) [*spt16/spt6Δ202 / WT*] (log$_2$ ratio)

1 2 3 4 5 6 7 8 9 10   1 2 3 4 5 6 7 8 9 10
highest   Rpb3   lowest   highest   Rpb3   lowest
enrichment   enrichment
in deciles   in deciles

C Top 200 genes with reduced Pol II in *spt16/spt6Δ202*

— WT   --- *SPT16/spt6Δ202*
--- *spt16/spt6Δ202*

Rpb3 occupancy

Rpb3 ChIP/Input (log$_2$ ratio)

TSS   TES

D 67 lowly expressed genes with reduced Pol II in *spt16/spt6Δ202*

p = 4.6 x 10^{-8}
p = 5.3 x 10^{-3}

Rpb3 ChIP/Input (log$_2$ ratio)

WT   *spt6*   *spt6Δ202*   *spt16*   *spt16 / spt6Δ202*

E 137 highly expressed genes with reduced Pol II in *spt16/spt6Δ202*

— WT   --- *SPT16/spt6Δ202*
--- *spt16/spt6Δ202*

H3 occupancy

H3 ChIP/Input (log$_2$ ratio)

-1000   TSS   +1000

F 67 lowly expressed genes with reduced Pol II in *spt16/spt6Δ202*

— WT   --- *SPT16/spt6Δ202*
--- *spt16/spt6Δ202*

H3 occupancy

H3 ChIP/Input (log$_2$ ratio)

-1000   TSS   +1000